Laminar characteristics of gyrencephaly using high resolution diffusion tensor imaging in vivo at 7T

Thursday, June 12, 2014: 12:45 PM - 2:45 PM
Congress Center Hamburg
Room: Hall H

Submission Number:

3875

On Display:

Wednesday, June 11 & Thursday, June 12

Authors:

Michiel Kleinnijenhuis[1,2,3], Tim van Mourik[1], David Norris[1,4,5], Dirk Ruiter[2], Anne-Marie van Cappellen van Walsum[2,1,5], Markus Barth[1,4]

Institutions:

[1]Radboud University Nijmegen, Donders Institute for Brain, Cognition and Behaviour, Nijmegen, Netherlands, [2]Department of Anatomy, Radboud university medical centre, Nijmegen, Netherlands, [3]Oxford Centre for Functional MRI of the Brain, University of Oxford, Oxford, United Kingdom, [4]Erwin L. Hahn Institute for Magnetic Resonance Imaging, Essen, Germany, [5]MIRA Institute for Biomedical Technology and Technical Medicine, University of Twente, Enschede, Netherlands

First Author:

Michiel Kleinnijenhuis - Lecture Information | Contact Me
Radboud University Nijmegen, Donders Institute for Brain, Cognition and Behaviour|Department of Anatomy, Radboud university medical centre|Oxford Centre for Functional MRI of the Brain, University of Oxford
Nijmegen, Netherlands|Nijmegen, Netherlands|Oxford, United Kingdom

Introduction:

Gyrification of the human cerebral cortex is a necessity for its extraordinary surface expansion that allows many more neurons as compared to other mammals. For neuroimaging, however, it complicates analysis. For example, it has long been established that cortical layers do not occupy the same depth in gyri and sulci [1]. Recently, *in vivo* [2] and *ex vivo* [5] diffusion imaging (DWI) has provided insights into the fibre architecture of the cortex, usually showing radial diffusion tensor (DT) orientations. This warrants investigation of the relation between cortical diffusion tensors and the gyral pattern.

Methods:

DWI and MP2RAGE were acquired from 5 subjects on a 7T system with a 32ch coil (Siemens, Erlangen, Germany). For DWI, a sagittal slab was acquired with 1 mm^3 voxels centered on the midline (RESOLVE [6]; 61 directions; b=1000 $s \cdot mm^2$; TR/TE=5800/56ms; 4 segments; FOV=212×212mm; matrix=212×212; 32-42 slices of 1mm; TA≈40-45 min). For MP2RAGE parameters were TR/TE=5000/2ms; TI1/TI2=0.9/3.2s; FOV=225×240mm; matrix=300×320; 224 slices of 0.75mm; TA=13 min. White/pial surfaces were reconstructed with FreeSurfer. Realignment and distortion correction [7] of DWI were performed with the Donders Diffusion toolbox. DWIs were resampled to 13 surfaces between the pial surface and a surface one cortical thickness T into white matter (WM). In white matter, equidistant surfaces were used (spacing: $1/6*T$). In grey matter (GM), equivolume sampling was used [8]. In our approach, sampling depth r as measured from the white surface was calculated by $r(f)=\sqrt[3]{(((R+T)^3-R^3)f+R^3)}-T$, where f=[0.17,0.33,0.5,0.66,0.83]; and $1/R$ and T are taken from the FreeSurfer curvatures and thickness. DT, mean diffusivity (MD), fractional anisotropy (FA) were calculated using Camino. Radiality was computed as the dot product between the cortex normal and the 1^{st} eigenvector of the DT [4]. Vertices were stratified in ten bins spanning the 10^{th},20^{th},…,100^{th} percentiles of curvature concatenated over all subjects.

Results:

MD (Figure 1a) is high at the pial surface and declines towards WM. In WM, FA (Figure 1b) increases from the crown to the fundus. The top GM surfaces have a low FA compared to the deep GM surfaces. In GM, diffusion tensors are predominantly radial (radiality > 0.5). Radiality is maximal for the 2^{nd} curvature bin of surface gm-2. The deep surfaces in the fundus are an exception, showing tangential diffusion tensors. In the WM under the fundus, DTs are also oriented tangential to the cortical sheet. In WM, there is a gradual increase in radiality from the bank to the crown. Radiality *under* the crown is lower than radiality *in* the crown. T1 (Figure1d) declines from pial surface to the WM. With the exception of the two deepest WM surfaces that show a peak under the bank, T1 does not vary with curvature consistently. However, it does show spatial variation (Figure 2).

Conclusions:

Diffusion tensor metrics vary with curvature as well as over cortical layers. T1 shows laminar dependence, but is stable over the curvature pattern. The patterns of diffusion tensors are in accordance with *ex vivo* diffusion MR microscopy and histological studies (Figure 3). For example, laminar differences in FA resemble previous ex vivo MR findings [3]. Tangential diffusion tensors with high FA under the fundus indicate densely packed u-fibres. Tangential fibres in deep cortical layers of the fundus are also seen in histology (* in Figure 3b) and suggest a very different fibre insertion pattern as compared to the crown. Partial volume effects are a potential confound, as might be seen in the laminar profile of MD. Our results indicate that the gyral pattern needs to be taken into account in high-resolution DWI.

Neuroanatomy:

Cortical Anatomy and Segregation

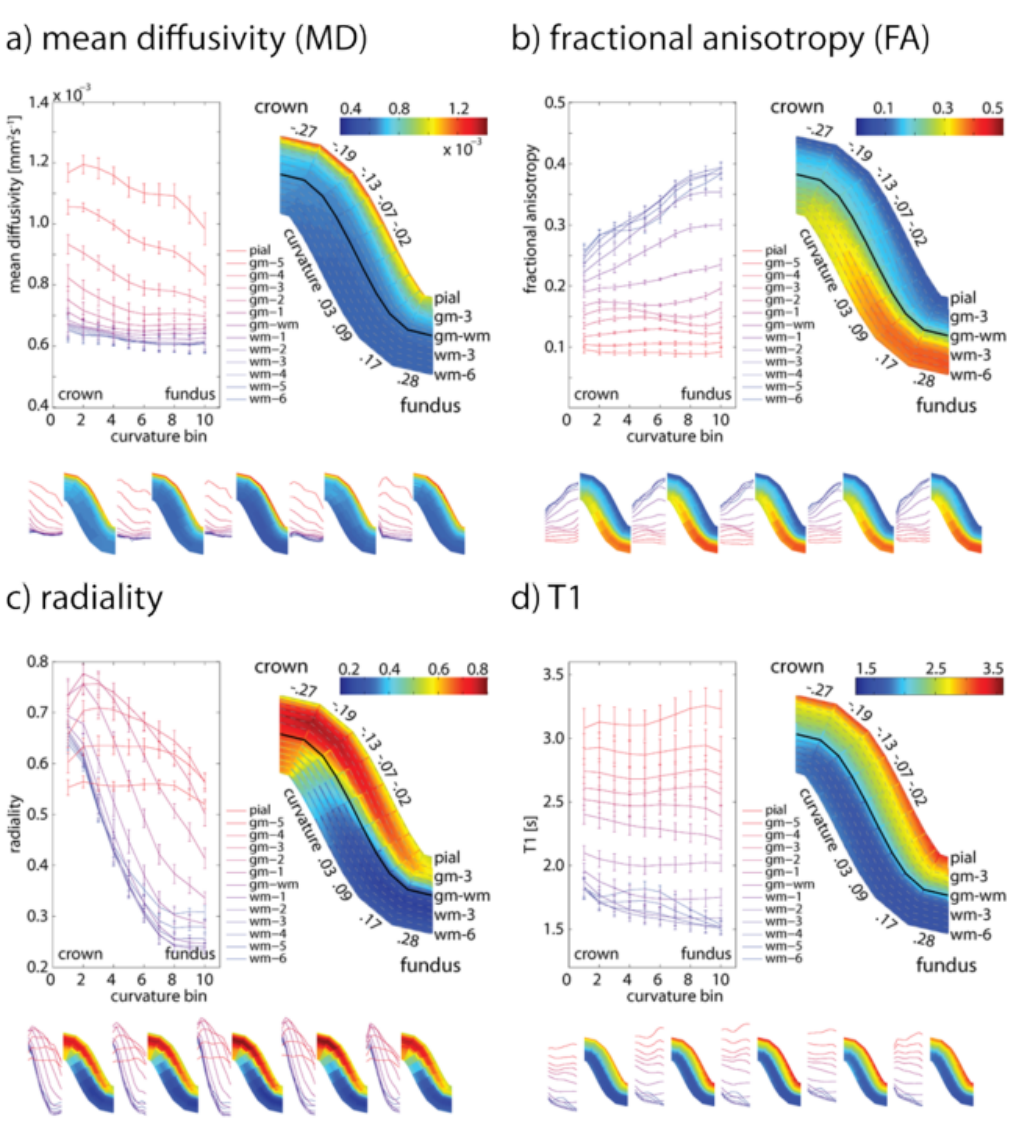

Figure 1. Mean diffusivity (a), fractional anisotropy (b), radiality (c) and T1 (d) values of the gyri of the medial wall of the hemispheres. The graphs show the values over the ten cortical curvature bins for each surface (traces red to blue for pial surface to the depth of the white matter). Error bars indicate standard deviation over subjects. The model gyrus represents the laminar and curvature dependence in colour-coded patches. The crown is on top, and the fundus on the bottom. The solid line in the middle represents the grey-white matter boundary; the grey dashed lines indicate the remaining surfaces. Note that the cortical surfaces are not equidistant. Numbers around the model show curvature values for the curvature bins (bin 1 and 10 go to -∞ and ∞, respectively) The lower rows in each panel show results (traces and patches) for the five individual subjects (scaling is identical to the average).
a) MD shows a laminar pattern with high MD at the pial surface and low MD near the GMWM boundary / in the WM. Variation with cortical curvature is less pronounced, but MD is higher in the crown than in the fundus for any (cortical) surface. b) In WM, FA increases from crown to fundus. The deepest WM layers have a dip in the profile (resembling the maximum for T1 in d), perhaps caused by sampling into the opposing bank). In GM, FA increases from the superficial layers to deep layers. FA in intermediate GM layers is relatively high on the crown as compared to the fundus. c) The radiality in WM is high under the crown, declining steeply over the bank, turning tangential under the fundus. This tangential orientation persists in the lower layers of the cortex in the fundus, while the remainder of the cortex is characterized by predominant radial diffusion tensors (the maximum radiality is in the 2nd curvature bin of layer gm-2). The T1 has a laminar pattern decreasing from pial surface to the gm-wm. No pronounced curvature dependence is seen.

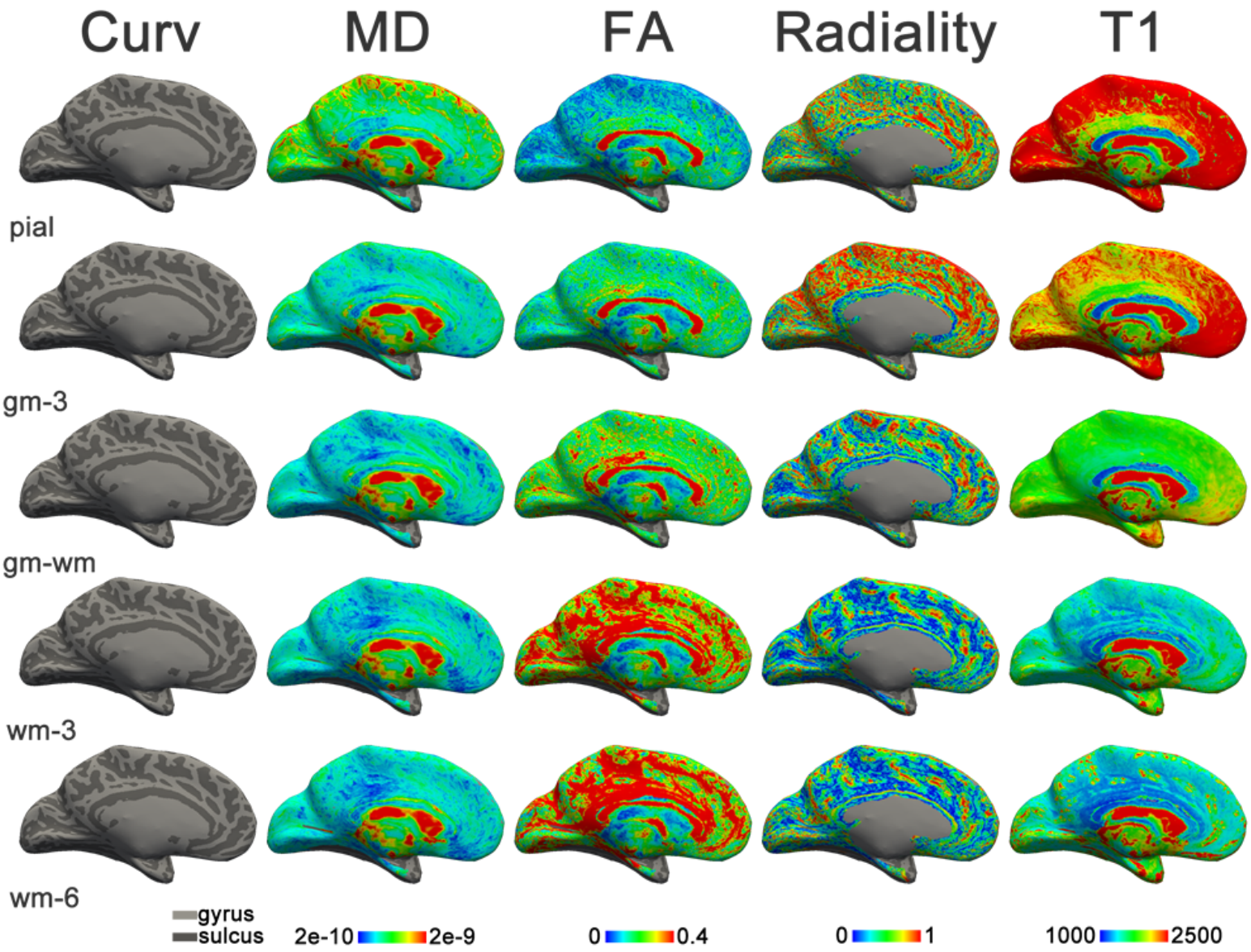

Figure 2. Spatial maps of the medial wall of the left hemisphere for subject1 for surfaces [pial, gm-3, gm-wm,wm-3, wm-6] in the different rows. Columns from left to right: the gyral sulcal pattern (Curv), the mean diffusivity (MD in 10^6 mm^2s^{-1}), the fractional anisotropy (FA), the radiality, and the T1 map (in ms). For MD, spatail variation is limited. FA, however, shows pronounced spatial variability in the WM under the cortical sheet (low FA under gyri, high FA under sulci). Radiality appears random at the pial surface. In the middle cortical surface (2nd row) the tensors are mostly radial (red)except for sulci, where the pattern is more random (green). For the gm-wm boundary and the WM surfaces, the spatial radiality pattern follows the gyral/sulcal pattern with tangential tensors in the fundi and radial tensors on the crowns. The spatial distribution of T1 values bears resemblance to FA, with hotspots for the posterior cingulate gyrus and the primary motor/somatosensory cortex.

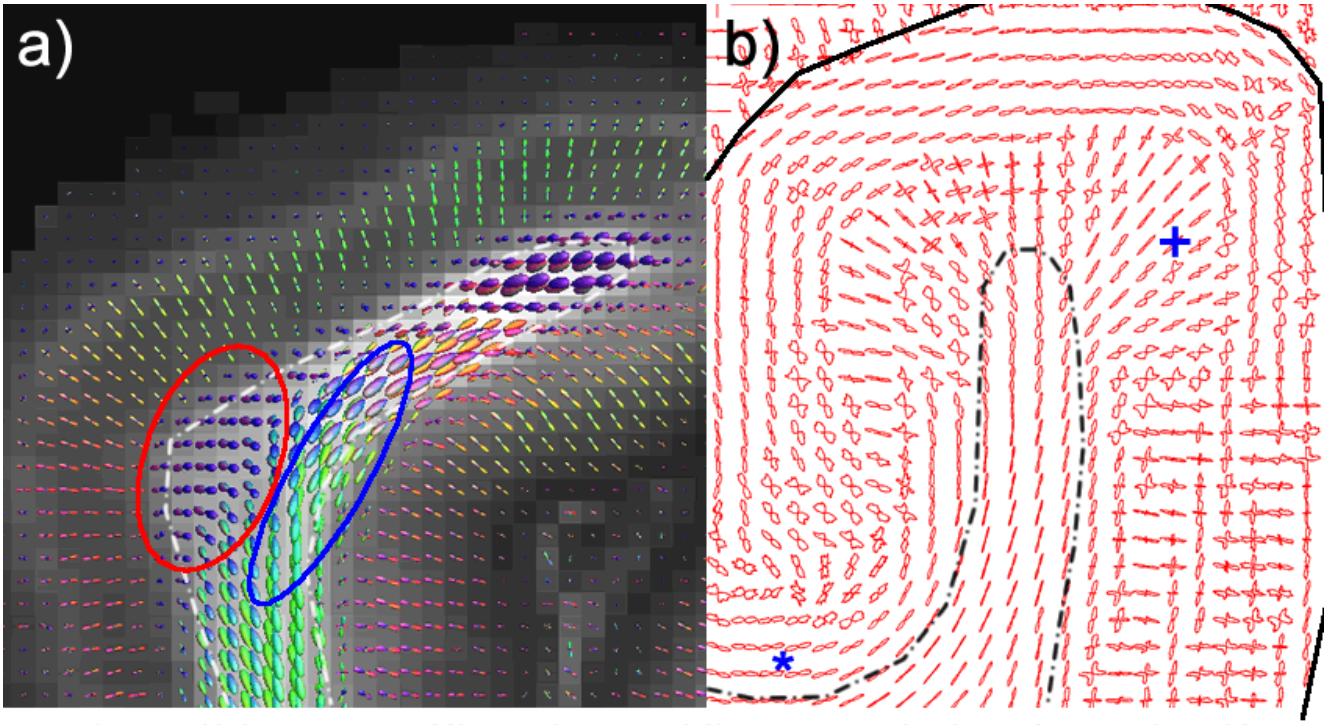

Figure 3. MR and light microscopy of fibres in the gyrus. a) fibre orientation distribution functions derived from ex vivo MR diffusion microscopy of the primary visual cortex. U-fibres in the concavity of the cortical fold are in the in-plane direction over the gyrus (blue ellipse), while u-fibres in the convexity are mostly directed along the length of the gyrus. The approximate grey-white matter boundary is drawn as a white dashed line. Radial fibres are found throughout the infragranular layers of the cortex. Adapted from [8]; b) histological fibre orientation distribution from the primary visual cortex. Asterisk (*) indicates dominant tangential orientation of the infragranular layers in the fundus of the sulcus. Plus (+) shows the region of maximal radiality of the fibres (note: away from the gyral crown).

Abstract Information

Would you accept an oral presentation if your abstract is selected for an oral session?

Yes

Please indicate below if your study was a "resting state" or "task-activation" study.

Other

Healthy subjects only or patients (note that patient studies may also involve healthy subjects):

Healthy subjects

Internal Review Board (IRB) or Animal Use and Care Committee (AUCC) Approval. Please indicate approval below. Please note: Failure to have IRB or AUCC approval, if applicable will lead to automatic rejection of abstract.

Yes, I have IRB or AUCC approval

Please indicate which method was used in your research:

Structural MRI

Diffusion MRI

For human MRI, what field strength scanner do you use?

7T

What post processing software packages do you use?

Free Surfer

References

Reference

[1] Bok S. (1929), 'Der Einfluß der in den Furchen und Windungen auftretenden Krümmungen der Großhirnrinde auf die Rindenarchitektur', Z Gesamte Neurol. Psychiatr., vol.12, pp. 682–750.
[2] Heidemann R.M. (2010), 'Diffusion imaging in humans at 7T using readout-segmented EPI and GRAPPA' Magnetic Resonance in Medicine, vol.64, pp. 9–14.
[3] Kleinnijenhuis M. (2013), 'Detailed laminar characteristics of the human neocortex revealed by NODDI and histology' Organization for Human Brain Mapping, Seattle, WA, USA, pp. 3815.
[4] McNab J.A. (2013), 'Surface based analysis of diffusion orientation for identifying architectonic domains in the in vivo human cortex', NeuroImage, vol.69, pp. 87–100.
[5] Miller K.L. (2012), 'Diffusion tractography of post-mortem human brains: optimization and comparison of spin echo and steady-state free precession techniques. NeuroImage', vol.59, pp. 2284–2297.
[6] Porter D.A. (2009) 'High resolution diffusion-weighted imaging using readout-segmented echo-planar imaging, parallel imaging and a two-dimensional navigator-based reacquisition', Magnetic Resonance in Medicine, vol.62, pp. 468–475.
[7] Visser E. (2012), 'Reference-free unwarping of EPI data using dynamic off-resonance correction with multiecho acquisition (DOCMA)', Magnetic Resonance in Medicine, vol.68, pp. 1247–1254.
[8] Waehnert M.D. (2013), 'Anatomically motivated modeling of cortical laminae', NeuroImage, doi:10.1016/j.neuroimage.2013.03.078